Commensuration of the antiferroelectric incommensurate phase in $Pb(Co_{1/2}W_{1/2})O_3$

S. Watanabe and Y. Koyama
Department of Materials Science and Engineering, and Kagami Memorial Laboratory for Materials Science and Technology, Waseda University, Nishiwaseda 2-8-26, Shinjuku-ku, Tokyo 169, Japan
(Received 20 July 2001; published 23 January 2002)

The antiferroelectric incommensurate phase in $Pb(Co_{1/2}W_{1/2})O_3$ is incommensurate in both wavelength and direction of the wave vector characterizing the modulation. In this study, the crystallographic features of the incommensurate and commensurate phases in $Pb(Co_{1/2}W_{1/2})O_3$ have been investigated by transmission electron microscopy to elucidate the details of commensuration to the commensurate phase. The wave vector of the modulation in the incommensurate phase was found to be $\mathbf{k}_I=[1-\delta_I\ 1-\delta_I\ \Delta_I]$ with $\delta_I\approx 0$ and $\Delta_I\approx 0$, while the wave vector in the commensurate phase is given by $\mathbf{k}_c=[1/2\ 1/2\ 0]$. The important features of the incommensurate and commensurate phases are that the modulation modes with $\mathbf{k}_1$ and $\mathbf{k}_{c1}$ are transverse atomic displacements of the Pb ions associated with the Σ_3 irreducible representation of the C_{2v} point group, and that another modulation with $\mathbf{k}_{c2}=[110]$ takes place in the commensurate phase. The $\mathbf{k}_{c2}$ modulation is associated with the X_{10} representation corresponding to the antiparallel displacement of the Pb ions. The appearance of the $\mathbf{k}_{c2}$ modulation is accompanied by that of a pseudoperiodic array of antiphase boundaries with a phase shift of π, and thus the commensurate phase is a nearly commensurate phase. That is, commensuration of both wavelength and direction of the incommensurate modulation takes place via the introduction of the X_{10} displacement with the antiphase boundaries. If the antiphase boundary is regarded as a discommensuration, the commensuration process of the antiferroelectric incommensurate phase to the commensurate phase is therefore characterized by the appearance of a discommensuration, not by its annihilation.

DOI: 10.1103/PhysRevB.65.064108 PACS number(s): 77.90.+k, 68.37.Lp, 64.70.Kb

I. INTRODUCTION

Commensuration in an incommensurate-to-commensurate transition is a process of recovery of the translational symmetry, which is broken in an incommensurate phase. According to McMillan's proposal,[1] local recovery of the translational symmetry takes place via the formation of a discommensurate structure. An incommensurate-to-commensurate transition is then characterized by the annihilation of dicommensurations.[2–8] With this proposal in mind, we have studied the crystallographic features of the commensuration process of the incommensurate phase in the complex perovskite oxide $Pb(Co_{1/2}W_{1/2})O_3$. However, the process of commensuration turned out to be different. In this paper, we describe and analyze the data obtained experimentally on the incommensurate and commensurate phases of this oxide.

$Pb(Co_{1/2}W_{1/2})O_3$ has a simple perovskite structure with ordering of the Co and W ions, both of which occupy the *B* site of the structure.[9] The crystal structure of the high-temperature phase above about 300 K does not basically include any atomic displacement and its space group is $Fm\bar{3}m$. When the temperature is lowered, the oxide undergoes two successive transitions: first to an antiferroelectric incommensurate phase around 300 K, and then to a commensurate orthorhombic phase around 235 K.[10] A monoclinic distortion is present in the intermediate-temperature incommensurate phase.[11,12]

Previous works on $Pb(Co_{1/2}W_{1/2})O_3$ have shown that the incommensurate phase is characterized by a modulated structure with a wave vector $k_I=\langle 1-\delta_I\ 1-\delta_I\ \Delta_I\rangle$,[10,12] in the $Fm\bar{3}m$ notation, where the values of δ_I and Δ_I are close to zero.[10] This shows that both the magnitude and the direction of the modulation are incommensurate in the incommensurate phase. The antiparallel displacement of the Pb ions, which is responsible for antiferroelectricity, was reported to play a major role in the modulation mode.[13] On the other hand, the low-temperature commensurate structure was found to have a wave vector $k_c=\langle 1/2\ 1/2\ 0\rangle$. Therefore, commensuration in $Pb(Co_{1/2}W_{1/2})O_3$ takes place in two factors: the magnitude and the direction of the modulation. Furthermore, the magnitude of the wave vector exhibits a large change from the quasi-zero value of δ_I to $\delta_c=1/2$. Although the commensurate phase was suggested to exhibit ferrielectricity,[14] the atomic displacement involved in the commensurate structure has not been determined yet. The presence of discommensuration in the commensurate phase was also pointed out by Randall *et al.*[15]

As mentioned above, the incommensurate-to-commensurate transition in $Pb(Co_{1/2}W_{1/2})O_3$ is characterized by commensuration of both the magnitude and the direction of the modulation. Our interest is focused on how the oxides makes an own effort for such a commensuration, and to understand it we have examined the crystallographic features of both commensurate and incommensurate phases by transmission electron microscopy. On the basis of the experimental data, we first analyze the atomic displacements in the incommensurate and commensurate phases and then discuss the characteristic features of commensuration in $Pb(Co_{1/2}W_{1/2})O_3$.

II. EXPERIMENTAL PROCEDURE

$Pb(Co_{1/2}W_{1/2})O_3$ samples used in the present work were prepared by a conventional solid state reaction. Powders of

PbO, CoO, and WO_3 were mixed for 16 h and pressed into pellets. The pellets were calcined at 850 °C for 10 h in air, then crushed, mixed for 16 h, and finally pressed again into pellets. The samples used in our study were obtained by sintering the pellets at 950 °C for 1 h in air. The crystallographic features of the samples were examined in the temperature range between 90 K and 373 K by taking electron diffraction patterns, and bright and dark field images. The study was carried out using H-8100 and JEM-3010 transmission electron microscopes operating at accelerating voltages of 200 kV and 300 kV, respectively, and equipped with cooling holders. Specimens for transmission electron microscopy observation were prepared by Ar-ion thinning. This oxide being insulating, each specimen was coated with a carbon film.

III. EXPERIMENTAL RESULTS

The present experimental data confirmed that $Pb(Co_{1/2}W_{1/2})O_3$ samples above about 300 K had the ordered perovskite structure with the $Fm\bar{3}m$ space group. Samples cooled from the high-temperature $Fm\bar{3}m$ phase transformed into the incommensurate phase around 300 K. Figure 1 shows three electron diffraction patterns taken from a sample at 290 K in the incommensurate phase. The electron incidences in (a), (b), and (c) are parallel to the $[\bar{1}11]$, $[1\bar{1}0]$, and $[\bar{2}03]$ directions, respectively. All diffraction spots are indexed in the $Fm\bar{3}m$ notation. In these patterns, satellite reflections are observed in the vicinity of the 110 positions in addition to the fundamental reflections due to the high-temperature $Fm\bar{3}m$ structure. In particular, the presence of 111 reflections is indicative of *B*-site ordering. The important features of the satellite reflections are that the locations of the reflections deviate from the $\langle 110 \rangle$ directions, and that higher-order reflections are clearly seen, as indicated by the arrow. The former feature implies that the modulation is incommensurate in both magnitude and direction. The wave vector of the incommensurate modulation, $\mathbf{k}_I = \langle 1 - \delta_I \; 1 - \delta_I \; \Delta_I \rangle$ with $\delta_I = 0.068$ and $\Delta_I = 0.045$, was determined on the basis of these patterns. The higher-order reflections are identified as diffraction harmonics showing that the modulation mode is due to atomic displacement. In addition, it was found that the satellite reflections along the $\langle 110 \rangle$ direction through the 000 origin arise from double diffraction. Thus the displacement should have a transverse-wave character. The incommensurate modulation was therefore confirmed to be a purely displacive modulation with a transverse-wave character.[13]

The features of the domain structure in the incommensurate phase were examined by taking dark field images using satellite reflections. Figure 2 shows two dark field images of the sample at 290 K, together with the corresponding $[\bar{2}03]$ electron diffraction pattern. In the pattern, the satellite reflections indicating the incommensurate modulation are clearly seen. The dark field image in (b) was taken using the satellite reflections in the vicinity of the 332 position in this pattern. The image in (c) is an enlarged image of the area surrounded

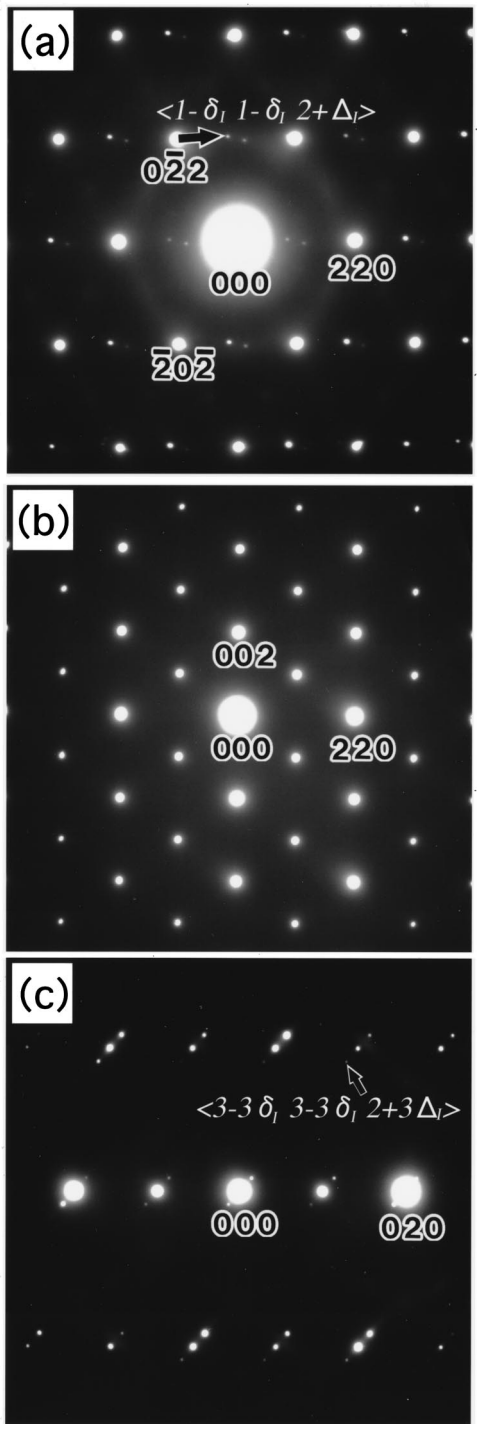

FIG. 1. Electron diffraction patterns of $Pb(Co_{1/2}W_{1/2})O_3$ at 290 K in the incommensurate phase. The electron incidences in (a), (b), and (c) are parallel to the $[\bar{1}11]$, $[1\bar{1}0]$, and $[\bar{2}03]$ directions, respectively.

by white lines in (b). In the image in (b), a dark-contrast band with a width of about 0.5 μm is observed. The interface between the dark- and bright-contrast regions is parallel to the (010) plane. In addition, fringes with a spacing of about 1.9 nm can be observed along the [332] direction in the bright-contrast region, as shown in the enlarged image. The spacing and the direction of the fringes obviously correspond

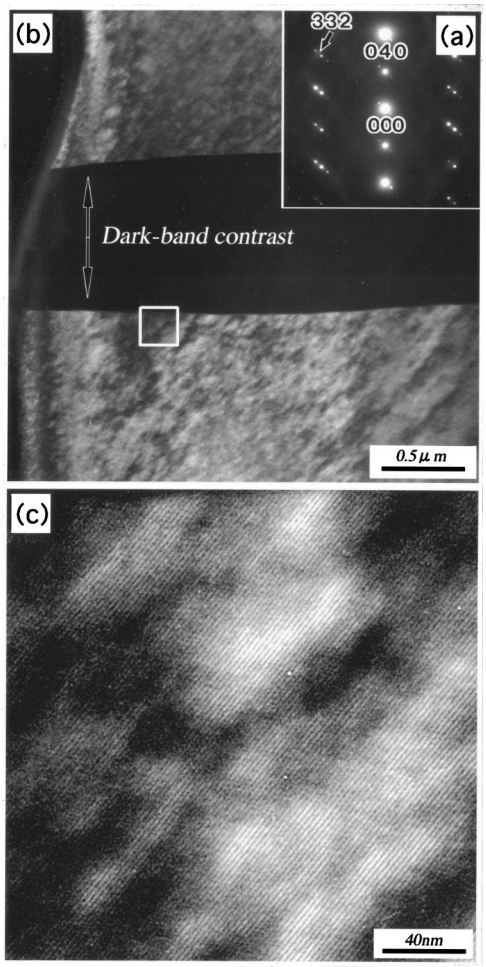

FIG. 2. Two dark field images of $Pb(Co_{1/2}W_{1/2})O_3$ at 290 K in the incommensurate phase, together with a corresponding $[\bar{2}03]$ electron diffraction pattern. The dark field images in (b) was taken using the satellite reflections in vicinity of the 332 position in the pattern. The image in (c) is an enlarged image of the area surrounded by white lines in (b).

to those between the satellite reflections used. As already reported,[11,12] a monoclinic distortion is present in the incommensurate phase. Thus the dark- and bright-contrast regions are assigned to two different monoclinic variants and the incommensurate structure is identified as a modulated structure characterized by the single wave vector $\mathbf{k}_I=[1-\delta_I\ 1-\delta_I\ \Delta_I]$. We also examined the intensities of the satellite reflections from a single monoclinic variant. In addition to the absence of the satellite reflection along the [110] direction through the origin, there was no satellite reflection in the $[1\bar{1}0]$ diffraction pattern, as will be shown in the case of the commensurate phase. We conclude thus that the eigenvector of the transverse modulation is almost parallel to the $[1\bar{1}0]$ direction and not to the [001] direction.

When the sample was cooled below 290 K, the incommensurate-to-commensurate transition occurred around 230 K. Three electron diffraction patterns of the sample at 90 K in the commensurate phase are shown in Fig. 3. The electron incidence is parallel to the [001], $[\bar{1}11]$, and

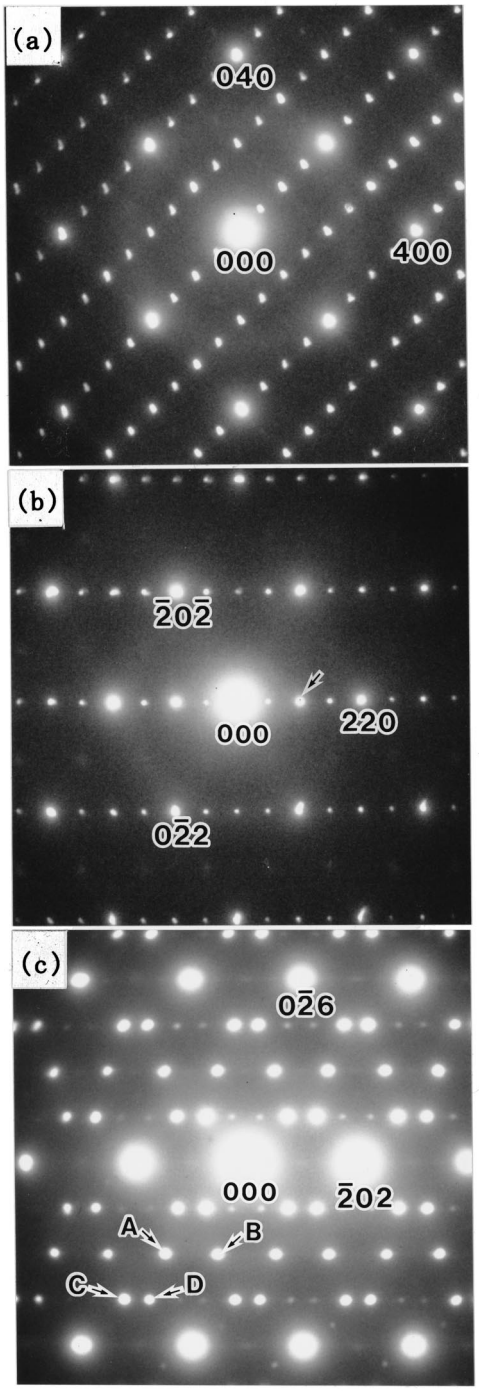

FIG. 3. Electron diffraction patterns of $Pb(Co_{1/2}W_{1/2})O_3$ at 90 K in the commensurate phase. The electron incidence is parallel to the [001], $[\bar{1}11]$, and [131] directions in (a), (b), and (c), respectively.

[131] directions in (a), (b), and (c), respectively. In addition to the fundamental reflections due to the high-temperature $Fm\bar{3}m$ structure, superlattice reflections are clearly seen at $\mathbf{k}_c=\langle 1/2\ 1/2\ 0\rangle$, together with reflections at the 110 positions, which are forbidden for the $Fm\bar{3}m$ structure. Furthermore, the intensity of the 110 forbidden reflections is stronger than that of the superlattice reflections, as indicated by the arrow in Fig. 3(b). This clearly shows that these 110

reflections are new reflections and not the second-order harmonic of the $\mathbf{k}_c=\langle 1/2\ 1/2\ 0\rangle$ superlattice reflection. In other words, the reciprocal space of the commensurate phase is characterized by the presence of both the $\mathbf{k}_c=\langle 1/2\ 1/2\ 0\rangle$ superlattice and 110 forbidden reflections.

In order to confirm the presence of the forbidden reflection and to understand the features of the domain structure in the commensurate phase, we took dark field images of the sample in the commensurate phase. Figure 4 shows four dark field images taken from the same area of the sample at 90 K. The corresponding [131] electron diffraction pattern was already shown in Fig. 3(c). Images in (a), (b), (c), and (d) were taken using the $11\bar{4}$ and $01\bar{3}$ forbidden and the $3/2\ 3/2\ \bar{6}$ and $1\ 3/2\ \overline{11/2}$ superlattice reflections indicated by *A*, *B*, *C*, and *D* arrows in Fig. 3(c). Contrasted bands are observed in these images. The interface between the bands is almost parallel to the (101) plane and the average width of the bands is about 100 nm. This contrast is obviously due to the orthorhombic distortion in the commensurate phase.[16] Each band corresponds to one orthorhombic variant. The characteristic features of these contrasted bands are that the bright and dark bands are reversed in the images for the forbidden reflections [Figs. 4(a) and 4(b)], and that some bright bands are missing in the superlattice images [Figs. 4(c) and 4(d)], as indicated by the α and β arrows. In order to understand an origin of this absence, we took dark field images of this area using other superlattice reflections. A domain structure in the commensurate phase, which was derived from the analysis of the dark field images, is schematically depicted in Fig. 5, together with a corresponding reciprocal lattice. In the reciprocal lattice, two forbidden reflections and four superlattice reflections with $\mathbf{k}_c=[1/2\ 1/2\ 0]$, $[0\ 1/2\ \overline{1/2}]$, $[1/2\ \overline{1/2}\ 0]$ and $[0\ \overline{1/2}\ \ \overline{1/2}]$ are denoted by $F1$, $F2$, $S1$, $S2$, $S3$, and $S4$, respectively. For instance, as shown in the domain structure, the domain indicated by α gives rise to the $S3$ and $F1$ reflections. That is, each orthorhombic variant produces both one superlattice and one forbidden reflection. The atomic displacement in the commensurate phase is therefore the superposition of two atomic displacements.

The extinction and the intensities of the superlattice and forbidden reflections from a single variant were examined to determine the nature of these two atomic displacements. Figure 6 shows two electron diffraction patterns taken from one orthorhombic variant in the commensurate phase. The electron incidences in (a) and (b) are parallel to the [001] and $[1\bar{1}0]$ directions, respectively. The pattern obtained with the [001] incidence exhibits superlattice and forbidden reflections, whereas only the fundamental reflections are present with the $[1\bar{1}0]$ incidence. From the latter result, we conclude that the superlattice and forbidden reflections along the [110] direction through the origin in Fig. 6(a) are due to double diffraction. Two displacements giving rise to the $\mathbf{k}_c=[1/2\ 1/2\ 0]$ superlattice and corresponding forbidden reflections can be identified as transverse waves with an eigenvector parallel to the $[1\bar{1}0]$ direction.

The features of the commensurate modulation were examined by taking lattice images of a single orthorhombic variant. A lattice image from a single variant at 90 K and the corresponding $[\bar{1}11]$ electron diffraction pattern are shown in Fig. 7, together with the calculated diffraction pattern produced from the image. The lattice image was taken with the $\overline{3/2}\ 1/2\ \bar{2}$, $\overline{1/2}\ 3/2\ \bar{2}$, and $\bar{1}\bar{1}\bar{2}$ reflections indicated by *A*, *B*,

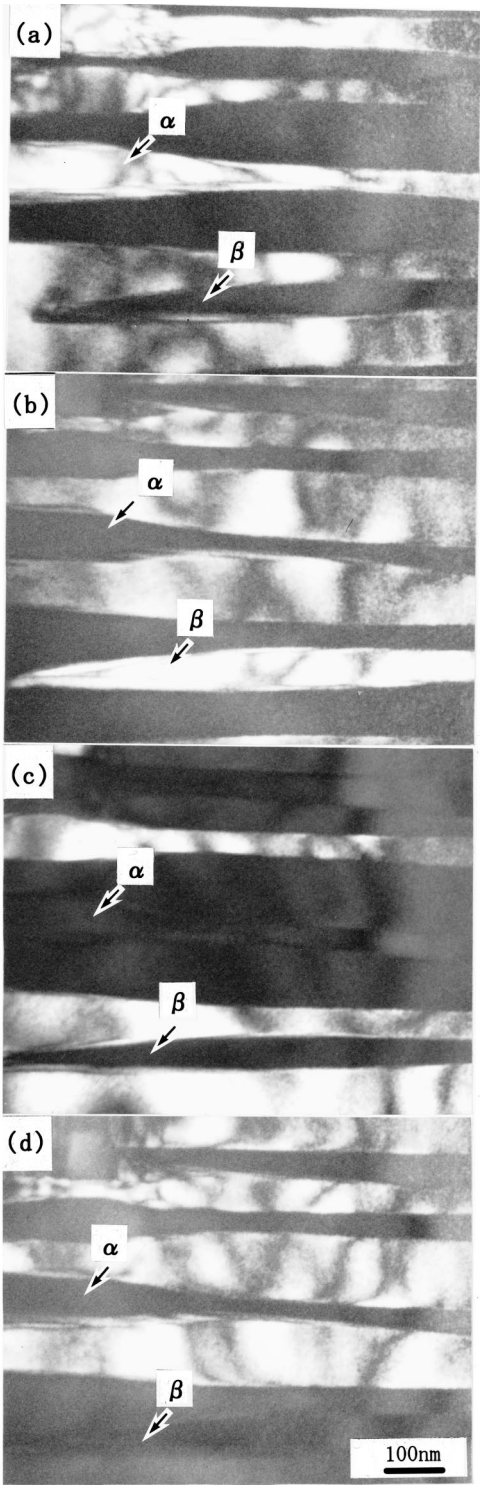

FIG. 4. Dark field images of the orthorhombic commensurate phase at 90 K. In all the images, the electron incidence is parallel to the [131] direction. Images in (a), (b), (c), and (d) were taken using the $11\bar{4}$ and $01\bar{3}$ forbidden and the $3/2\ 3/2\ \bar{6}$ and $1\ 3/2\ \overline{11/2}$ superlattice reflections indicated by *A*, *B*, *C*, and *D* arrows in Fig. 3(c).

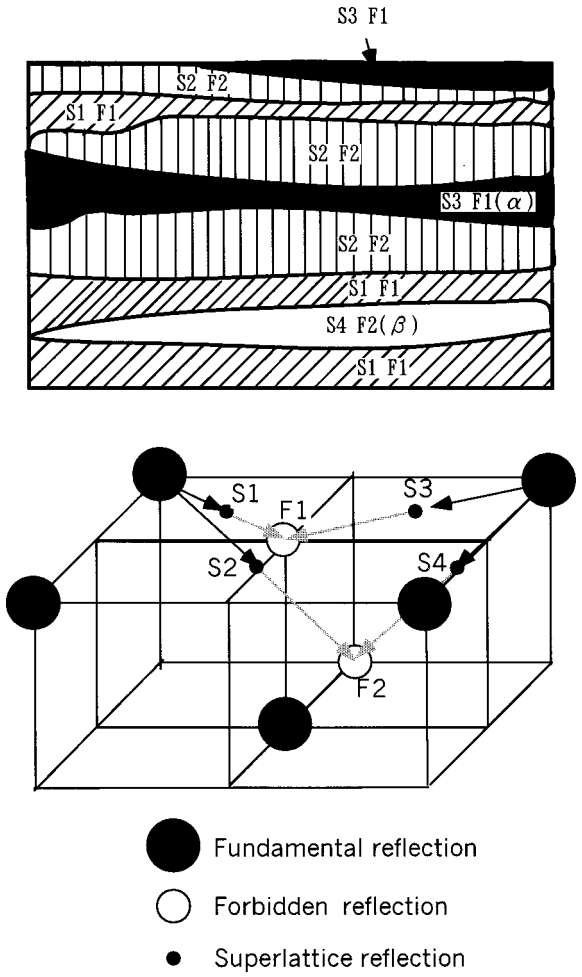

FIG. 5. Schematic diagram showing the domain structure of the commensurate phase, derived from the analysis of the dark field images, together with a corresponding reciprocal lattice. The details of the figure are described in the text.

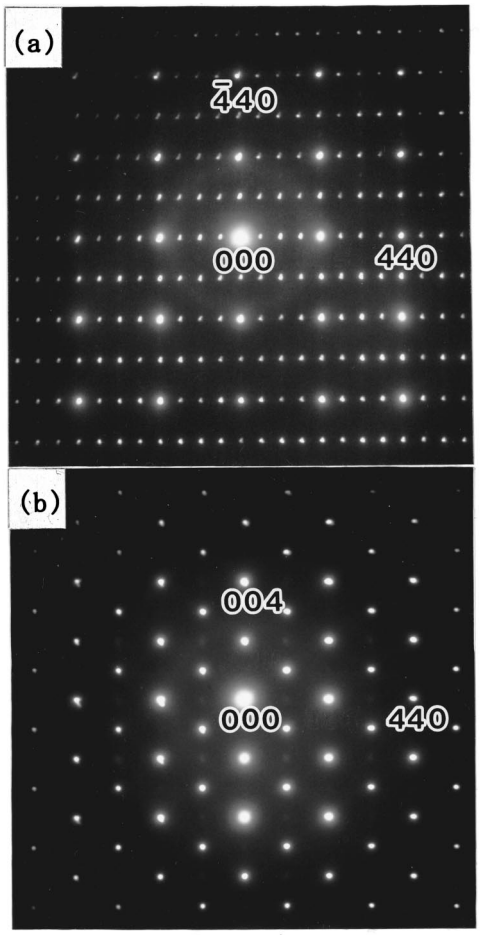

FIG. 6. Electron diffraction patterns taken from one orthorhombic single variant of the commensurate phase at 90 K. The electron incidence in (a) and (b) is parallel to the [001] and $[1\bar{1}0]$ directions, respectively.

and *C* arrows in Fig. 7(a). In the image, we can see not only lattice fringes along the [110] direction, but also a pseudoperiodic array of dark bands almost aligned with the [514] direction. The spacing of the fringes and the bands is about 1.1 nm and 18 nm, respectively. The fringe spacing is obviously the inverse of the magnitude of $\mathbf{k}_c=[1/2\ 1/2\ 0]$ and the pseudoperiodic array of the dark bands is confirmed as the splitting of the superlattice reflections, as shown by the arrow in the calculated pattern. The most important feature of the image is the phase shift of π in the lattice fringes across one dark band. Thus the dark band can be assigned to an antiphase boundary with a phase shift of π, which is associated with the commensurate modulation. This clearly shows that, below about 300 K, $Pb(Co_{1/2}W_{1/2})O_3$ does not have a commensurate structure, but strictly a nearly commensurate structure.

IV. DISCUSSION

The present experimental data on $Pb(Co_{1/2}W_{1/2})O_3$ show that the antiferroelectric incommensurate phase with a monoclinic distortion is characterized by a purely displacive modulation with a transverse-wave character. The wave vector and the eigenvector of the modulation are given by $\mathbf{k}_I=[1-\delta_I\ 1-\delta_I\ \Delta_I]$ with $\delta_I\approx 0$ and $\Delta_I\approx 0$ and **e** about parallel to $[1\bar{1}0]$ direction, respectively. Thus both the magnitude and the direction of the wave vector are incommensurate and commensuration in $Pb(Co_{1/2}W_{1/2})O_3$ involves both the magnitude and the direction of the modulation. On the other hand, we found that the low-temperature phase usually accepted as a commensurate orthorhombic phase has, in fact, strictly a nearly commensurate structure. The atomic displacement involved in its crystal structure is basically a superposition of two transverse displacements with $\mathbf{e}//[1\bar{1}0]$, which wave vectors can be expressed as $\mathbf{k}_N=[1-\delta_N^i\ 1-\delta_N^i\ \Delta_N^i]$. For the displacement denoted by $i=1$, the values of δ_N^i and Δ_N^i are $\delta_N^1\approx 1/2$ and $\Delta_N^1\approx 0$ while for $i=2$, $\delta_N^2\approx 0$ and $\Delta_N^2\approx 0$. Furthermore, the deviation from the commensurate wave vector arises from the pseudoperiodic array of antiphase boundaries associated with these displacements. In other words, the nearly commensurate phase consists of commensurate regions separated by antiphase boundaries. Based on these experimental data, we will now confirm the atomic displacement in the incommensurate phase and deter-

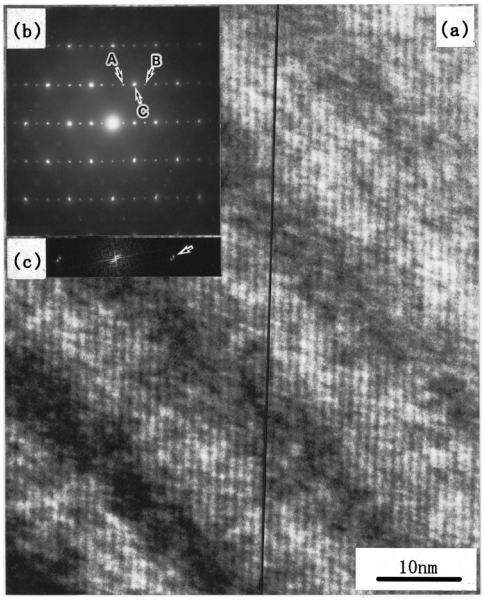

FIG. 7. (a) Lattice image of one orthorhombic single variant at 90 K and (b) the corresponding $[\bar{1}11]$ electron diffraction pattern, together with (c) the calculated diffraction pattern produced from the lattice image. The lattice image was taken using the $\overline{3/2\ 1/2\ 2}$, $\overline{1/2\ 3/2\ 2}$, and $\bar{1}1\bar{2}$ reflections indicated by *A*, *B*, and *C* arrows in (b).

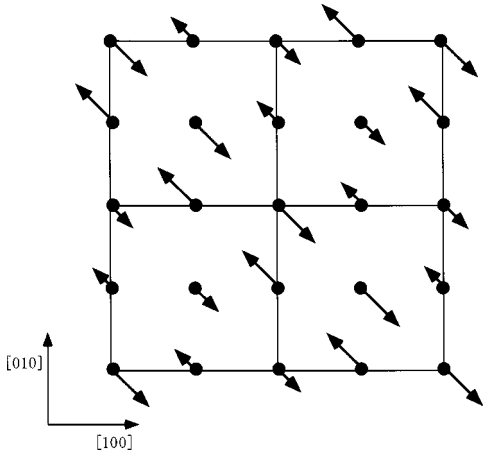

FIG. 8. Atomic displacement of the Pb ions in the commensurate region produced by a superposition of the Σ_3 and X_{10} atomic displacements. The arrows shown in the figure represent the resultant shifts of the Pb ions.

mine the atomic displacement in the commensurate region of the nearly commensurate phase. Finally, the characteristic features of the transition to the nearly commensurate phase will be discussed.

The atomic displacements in the nearly commensurate phase as well as in the incommensurate phase are analyzed by taking into account the allowed phonon modes in the $Fm\bar{3}m$ structure. Concerning the displacement in the incommensurate phase, our experimental data show that the wave vector of the incommensurate modulation is $\mathbf{k}_I=[1-\delta_I\ 1-\delta_I\ \Delta_I]$ with $\delta_I\approx 0.068$ and $\Delta_I\approx 0.045$ at 290 K. This modulation can then be due to the condensation of a phonon mode with $q=[\xi\xi 0]$ in the $Fm\bar{3}m$ structure. The point group of the $[\xi\xi\ 0]$ symmetry is C_{2v}, which has four irreducible representations called Σ_1, Σ_2, Σ_3, and Σ_4. Concerning the modulation mode, on the other hand, modulation occurs by means of a transverse wave with an eigenvector almost parallel to the $[1\bar{1}0]$ direction. Thus the Σ_3 representation is responsible for the atomic displacement in the incommensurate phase. The major feature of the displacement derived from the Σ_3 representation is the antiferroelectric displacement of the Pb ion. This is consistent with the displacement reported by Bonin *et al.*[13]

As mentioned above, the nearly commensurate phase consists of commensurate regions separated by antiphase boundaries. Thus the incommensurability in the nearly commensurate phase arises from the pseudoperiodic array of boundaries. The determination of the atomic displacement in the commensurate region follows from the analysis of our data showing that there are two transverse displacements in the nearly commensurate phase. The first one denoted by $i=1$ in the commensurate region, has a commensurate wave vector $\mathbf{k}_{c1}=[1/2\ 1/2\ 0]$, while the wavelength of the other one, denoted by $i=2$, is just the (110) lattice spacing. These two displacements have the same eigenvector parallel to the $[1\bar{1}0]$ direction. Therefore the $i=1$ displacement results from the condensation of the phonon mode associated with the Σ_3 representation in the $Fm\bar{3}m$ structure. The $i=1$ displacement is then the same as that in the incommensurate phase. As for the $i=2$ displacement, on the other hand, the most appropriate representation should be the two-dimensional X_{10} representation at the X point.[17] The $i=2$ displacement derived from the X_{10} representation is obviously the antiparallel shift of the Pb ions. Figure 8 shows the resultant displacement of the Pb ions in the commensurate region, which was obtained by the superposition of the Σ_3 and X_{10} displacements. In the superposition, we assumed that the nodes of the Σ_3 displacement were located at those of the X_{10} displacement, and that the magnitude of the former displacement was smaller than that of the latter. The assumption on the magnitude is based on the fact that the intensity of the superlattice reflection due to the Σ_3 displacement is weaker than that of the X_{10} forbidden reflection. As shown by the diagram, the resultant displacement of the Pb ions is made of two groups of antiparallel shifts of different magnitudes. With this type of displacement, the nearly commensurate phase of $Pb(Co_{1/2}W_{1/2})O_3$ is neither antiferroelectric nor ferrielectric, and some unique dielectric property must be expected.

We can now turn to the discussion of the characteristic features of the transition from the incommensurate phase to the nearly commensurate phase. As pointed out earlier, the commensuration in $Pb(Co_{1/2}W_{1/2})O_3$ occurs with a change of both the magnitude and the direction of the modulation. Because the Σ_3 displacement is involved in both the incommensurate and nearly commensurate phases, the modulation mode in these phases is identified as the Σ_3 displacement. In other words, the introduction of the X_{10} displacement with the pseudoperiodic array of antiphase boundaries produces

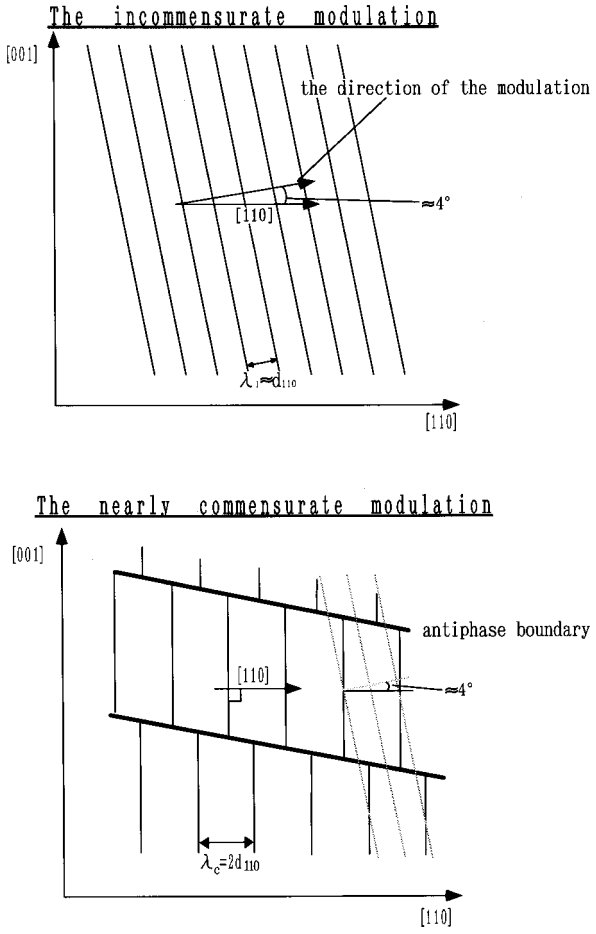

FIG. 9. Modulations in the incommensurate and nearly commensurate phases. The details of both modulations are described in the text.

the change in the wave vector of the Σ_3 displacement and results in a nearly commensurate phase instead of a commensurate phase. The modulations in the incommensurate and nearly commensurate phases are schematically depicted in Fig. 9. This figure represents the cross-section of the plane on which the magnitude and the direction of the shifts of the Pb ions are identical. In the incommensurate phase, the modulation is along a direction about 4° from [110] and has a periodicity close to the d_{110} lattice spacing. In the nearly commensurate phase, on the other hand, commensurate regions with a periodicity of $2d_{110}$ along the [110] direction are separated by antiphase boundaries, which are arranged pseudoperiodically along a direction close to [514]. Thus as reported first by Randall *et al.* for this oxide,[15] it seems that the antiphase boundary can be regarded as a discommensuration, although this is not strictly true. In fact, the discommensuration is characterized by a phase slip, which results in the change of only the magnitude of the modulation. The introduction of antiphase boundaries is therefore required to change both the magnitude and the direction of the modulation. If the discommensuration is defined here as a boundary separating commensurate regions, the commensuration in $Pb(Co_{1/2}W_{1/2})O_3$ is characterized by the appearance of this discommensurations. This is obviously different from the McMillan's proposal, mentioned earlier. We believe that commensuration in $Pb(Co_{1/2}W_{1/2})O_3$ is a new process for the recovery of the translational symmetry broken in the incommensurate phase.

V. CONCLUSION

The commensuration of the antiferroelectric incommensurate phase in $Pb(Co_{1/2}W_{1/2})O_3$ occurs with a change of both the wavelength and the direction of the wave vector characterizing the incommensurate modulation. The present experimental data showed that the modulation in the incommensurate and commensurate phases is a Σ_3 displacement, and that commensuration occurs with the introduction of a X_{10} displacement and of a pseudoperiodic array of antiphase boundaries with a phase shift of π. If the antiphase boundary is regarded as a discommensuration, then commensuration is accompanied by the introduction of a discommensuration. As a result, the commensurate phase is therefore strictly a nearly commensurate phase, in which the commensurate regions are separated by discommensurations, which are the antiphase boundaries.

ACKNOWLEDGMENT

The authors would like to thank H. Sato of Waseda University for providing good $Pb(Co_{1/2}W_{1/2})O_3$ samples.

[1] W. L. McMillan, Phys. Rev. B **14**, 1496 (1976).
[2] K. K. Fung, S. McKernan, J. W. Steed, and J. A. Wilson, J. Phys. C **14**, 5417 (1981).
[3] C. H. Chen, J. M. Gibson, and R. M. Fleming, Phys. Rev. B **26**, 184 (1982).
[4] J. Mahy, J. Van Landauyt, and S. Amelinckx, Phys. Rev. Lett. **55**, 1188 (1985).
[5] Y. Fujino, H. Sato, M. Hirabayashi, E. Aoyagi, and Y. Koyama, Phys. Rev. Lett. **58**, 1012 (1987).
[6] S. Mori, Y. Koyama, and Y. Uesu, Phys. Rev. B **49**, 621 (1994).
[7] Y. Koyama and M. Ishimaru, Phys. Rev. B **41**, 8522 (1990).
[8] Y. Koyama and S. Mori, Phys. Rev. B **44**, 7852 (1991).
[9] V. A. Bokov, S. A. Kizhaev, I. E. Myl'nikova, and A. G. Tutov, Sov. Phys. Solid State **6**, 2419 (1965).
[10] Ph. Sciau, G. Calvarin, B. N. Sun, and H. Schmid, Phys. Status Solidi A **129**, 309 (1992).
[11] W. Brixel, M. L. Werk, P. Fishcer, W. Buhrer, J.-P. Rivera, P. Tissot, and H. Schmid, Jpn. J. Appl. Phys. **24**, 242 (1985).
[12] Ph. Sciau, K. Krusche, P.-A. Buffat, and H. Schmid, Ferroelectrics **107**, 235 (1990).
[13] M. Bonin, W. Paciorek, K. Schenk and G. Chapuis, Acta Crystallogr., Sect. B: Struct. Sci. **51**, 48 (1995).
[14] H. Kim, B. Lee, and W. Choo, Ferroelectrics **125**, 223 (1992).
[15] C. A. Randall, S. A. Markgraf, A. S. Bhalla, and K. Baba Kishi, Phys. Rev. B **40**, 413 (1989).
[16] Ph. Sciau, P.-A. Buffat, and H. Schmid, Phase Transitions **31**, 45 (1991).
[17] G. Baldinozzi, Ph. Sciau, and A. Bulou, J. Phys.: Condens. Matter **7**, 8109 (1995).